European Journal of Agronomy 146 (2023) 126825

Contents lists available at ScienceDirect

European Journal of Agronomy

journal homepage: www.elsevier.com/locate/eja

Earlier sowing combined with nitrogen fertilization to adapt to climate change effects on yield of winter wheat in arid environments: Results from a field and modeling study

Hossein Moghaddam [a], Mostafa Oveisi [a], Mostafa Keshavarz Mehr [a], Javad Bazrafshan [c], Mohammad Hossein Naeimi [a], Behnaz Pourmorad Kaleibar [a], Heinz Müller-Schärer [a,b,*]

[a] Department of Agronomy and Plant Breeding, College of Agriculture and Natural Resources, University of Tehran, Karaj, Iran
[b] Department of Biology, University of Fribourg, Fribourg, Switzerland
[c] Department of Irrigation and Reclamation Engineering, College of Agriculture and Natural Resources, University of Tehran, Karaj, Iran

ARTICLE INFO

Keywords:
Arid region cropping system
Early sowing
General circulation model
Representative concentration pathway
APSIM-wheat simulation

ABSTRACT

Climate change effects on crop production are of high concern in arid regions that are suffering from increased drought. We parameterized the APSIM-Wheat (The Agricultural Production Systems sIMulator) model using data of two field experiments conducted in 2017 at two locations (Karaj and Khomein) in Iran differing in temperature and precipitation. The experiment was a split plot with four replications. Main plots measured 17 m by 5 m with four irrigation regimes of full irrigation (I_1), deficit irrigation from grain filling ($I_{2,}$), from beginning of flowering (I_2), and during the whole growth period (I_4). Sub-plots measured 3 m by 5 m with nitrogen (N) levels of 200 (N_1), 100 (N_2) and 50 (N_3) kg/ha of urea (46 % N). N_1 resulted in highest wheat biomass, grain yield, harvesting index and leaf area index (LAI), with the differences between the N levels decreasing with increasing water deficit period. The model was parameterized for both localities with data of treatment I_1 +N_1, then evaluated over 11 combinations of irrigation and nitrogen rates. Root mean square of errors (RMSE) were 0.3 and 0.15 t/ha for wheat biomass and grain yield, and 3.54 days for wheat phenology and 0.28 for LAI simulations. After model calibration, we ran the model with 20 general circulation models (GCMs) under two representative concentration pathways (RCP 4.5 and RCP 8.5), and crop production was projected for three future time periods. For 2010–2039, models simulate a marginal increase in wheat yield, however, with 2040–2069 and 2070–2099, most models simulate a decreased growing season length and grain yield. Nitrogen application was found to decrease the drought impact. Additionally, model simulation suggests that earlier sowing time and excessive irrigation are of benefit in adapting to climate change impact. Thus, in arid environments where additional irrigation is not an option, increased nitrogen application in combination with an earlier sowing time could be an effective adaptation strategy for future wheat production.

1. Introduction

The globally averaged combined land and ocean surface temperature data calculated as a linear trend show a warming of 0.85 °C (0.65–1.06) over the period 1880–2012, for which multiple independently produced datasets exist (Pachauri et al., 2014). The trend is projected to rise over the next 80 years under all assessed emission scenarios (van Vuuren and Carter, 2014). While climate change causes more intense and frequent precipitation in some regions (Barros et al., 2015), the areas such as Middle East and Africa are expected to suffer from significant drought, (Lange, 2019). Major crops such as wheat (*Triticum aestivum* L.), rice (*Oryza sativa* L.) and maize (*Zea mays* L.) in tropical and temperate regions will encounter restrictions of cultivation or suffer important yield losses (Korres et al., 2016). To adapt to climate change impacts, crop managers need to adopt innovative crop managements measures to maintain the sustainability of crop production under limited water supply condition.

Crop models that simulate crop response to meteorological, edaphic and biological factors (Montesino-San Martín et al., 2014) are used by decision makers as important tools for discovering sensitive points and

* Correspondence to: Department of Agronomy and Plant Breeding, University of Tehran, Karaj, Iran.
E-mail address: heinz.mueller@unifr.ch (H. Müller-Schärer).

https://doi.org/10.1016/j.eja.2023.126825
Received 21 December 2022; Received in revised form 27 February 2023; Accepted 27 March 2023

choosing adaptation strategies (Shi et al., 2013; Asseng et al., 2015). However, there are sources of uncertainty about the most appropriate choice of climate models and greenhouse gas emissions scenarios (Araya et al., 2015). Impact assessments based on multi-model climate projections are assumed to provide a more representative range of climate change impacts than single-model approaches (Tao et al., 2009; Najafi and Moradkhani, 2015).

Central and eastern Iran, a model area for arid environments of wheat production (Ministry of Agriculture-Jahad, 2014; Khosravi et al., 2014; Akbari et al., 2019), is frequently experiencing severe drought that force fundamental changes in cropping patterns and management. Average wheat production from this area is about 178,000 ton per year (Ministry of Agriculture-Jahad, 2019). One centigrade increase in temperature may decrease wheat yield by 5–7 %, and a 5 mm decrease in rainfall may cause 3 %– 9 % wheat yield loss (Pirttioja et al., 2015).

Here, we set out to parametrize the APSIM-Wheat model using field experimental data from two locations in central Iran, and then simulate climate change impact on wheat growth and yield. Using local meteorological data and the results of the field experiments assessing the effects and interactions of nitrogen fertilization and water shortage on wheat performance, we specifically ask (1) how do General Circulation Models (GCMs) forecast the regional climate change; (2) how does a moderate or a pessimistic scenario of climate change affect wheat growth and yield; (3) how might wheat be influenced by water shortage over future short-, medium- and long-term periods; and (4) are there crop management solutions, such as fertilization or sowing time, to

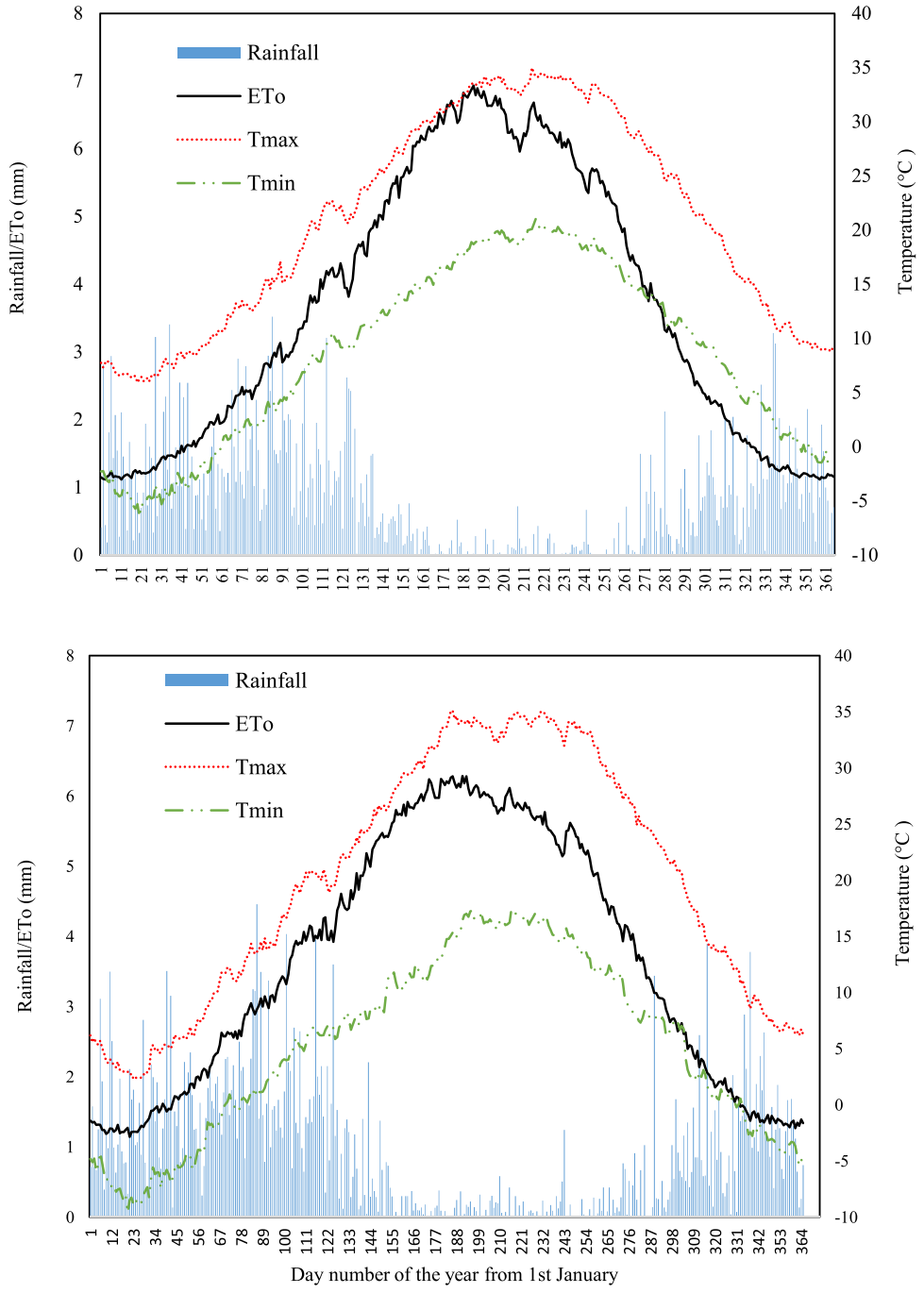

Fig. 1. Long-term (1980–2009) daily mean rainfall, reference evapotranspiration (ETo), and maximum (T_{max}) and minimum (T_{min}) temperature for Karaj (a) and Khomein (b).

alleviate climate change impacts on wheat yield?

2. Material and methods

2.1. Study locations

Field experiments were carried out at two locations in Iran during 2017 at Karaj (50° 57' E and 35° 48' N) and Khomein (50° 04′ E 33 ° 38′ N). Both locations have annual rainfall below 250 mm and are thus, classified as arid zones based on FAO criteria (FAO: Food and agriculture organization, 2018). Minimum and maximum temperatures, precipitation and evapotranspiration of the study locations are shown in Fig. 1.

2.2. Field experiments

We conducted field experiments in a split plot arrangement of treatments with four replications (blocks). Main plots measuring 17 m by 5 m represent four levels of irrigation consisting of full irrigation based on wheat water requirement (I_1) and deficit irrigation (60 %) from the beginning of grain filling (I_2), from the beginning of flowering (I_3), and during the whole growth period (I_4). Sub-plots measured 3 m by 5 m with nitrogen levels of 200 (N_1), 100 (N_2) and 50 (N_3) kg ha^{-1} of urea (46 % N). Therefore, each block consisted of four main plots differing in irrigation, and each main plot was split into three sub-plots differing in fertilizer level. Nitrogen fertilizer was broadcasted as topdressing at stem elongation of wheat. We installed main plots with 5-meter distance to avoid moisture penetration from adjacent main plots. Wheat (c. Sivand) was sown at a density of 400 plants/m^2 in mid-November and late October at the Karaj and Khomein sites, respectively. This corresponds to the commonly used planting density, although higher densities are also recommended especially for weed control (Jamali et al., 2017). The soil was shallow and well-drained silty loam for Karaj and sandy loam for Khomein with topsoil (0–0.3 m) bulk density of 1.47 and 1.6 g cm^{-3}, respectively. The soil physical and chemical characteristics are presented in Table 1. The soil was disked, leveled to reach a uniform texture and harrowed to smoothen it before planting. Wheat seeds were sown using a seed drill with row intervals of 17 cm. Each sup-plot consisted of 17 wheat rows and irrigation tapes were located next to each crop row for dripping irrigation. The space between drippers on the pipe was 15 cm, resulting in an infiltration surface of 17 × 15 cm area irrigated by the four rectangularly arranged drippers. We calculated the water requirement of wheat during the growing period (https://www.fao.org/3/u3160e/u31 60e04.htm) using the following formula (Fao.org):

$$\text{ETcrop} = \text{kc x Eto} \quad (1)$$

where ETcrop is the water requirement of a given crop in mm per unit of time e.g. mm/day, mm/month or mm/season and kc is the crop factor. For Eto calculation, we used a Class A evaporation pan installed next to the experimental fields. The pan evaporation rate i.e., Epan (mm/24 h) was multiplied by a Pan Coefficient (Kpan) as follows:

$$\text{ETo} = \text{Epan x Kpan} \quad (2)$$

We used an average of 0.70 for the Kpan. A season average crop factor (kc) of 1.20 was also used for wheat (López-Urrea et al., 2009), allowing to calculate the water requirement for wheat per day. We also installed a water meter on each main pipe that branched out to each main plot and irrigation was applied according to the calculated water requirement. Water requirement for wheat was calculated as 750 m^{-3} ha^{-1} for both experimental locations that are in an arid area. As the average temperature in the area was between 25 and 33 °C during the wheat flowering and grain filling in the study locations, the water requirement was between 6 and 7.6 mm per day (Scherer and Steele, 2019). The irrigation intervals were 5–7 days according to evaporation pan data (about 42–50 mm per irrigation).

We measured the leaf area of wheat using a LI-3000 C Portable Leaf Area Meter in each plot, and calculated LAI accordingly. We also measured the days for the phenological stages included in APSIM-wheat (Zhao et al., 2014). At maturity, we hand-harvested wheat in a 2 m^2 area in the middle of each plot, and subsequently measured wheat biomass and grains yield.

2.3. Statistical analyses

We tested the normality of the field data and their homogeneity of variances using Shapiro–Wilk test and Bartlett's test, respectively. To assess the treatment effects on wheat performance data, we used mixed ANOVA with location and its interaction with treatments as random effects, and irrigation, nitrogen effects and their interactions as fixed effects. Mean separation of treatments was done using protected LSD (least significant difference) test. All statistical analyses were performed using R-studio software (version 4.2.0) and package "Agricolae"(de Mendiburu and de Mendiburu, 2019)).

2.4. Climatic data and scenarios

Future climate scenario analysis was based on 30 years (1980–2009) weather data from each region. Data of long-term (1980–2009) daily rainfall, maximum temperature (T_{max}), minimum temperature (T_{min}) and solar radiation (R_s) were provided from the Karaj and Khomein meteorological stations (located at less than one kilometer from the experimental fields). Daily reference evapotranspiration (ETo) (1980–2009) was also calculated from temperature data (Hargreaves and Samani, 1985). Less than 3 % of the rainfall data in Karaj and 10 % of solar radiation data in Khomein were missing. Missing daily data were filled using The Modern-Era Retrospective Analysis for Research and Applications (MERRA) dataset that is provided by agricultural model intercomparison and improvement project (AgMIP) (AgMIP, 2013a,b) and climate team (Ruane et al., 2015). Site-specific climatic scenarios were generated using the CMIP5 GCM delta scenario technique with climate scenario generation tools ("R" scripts were used to prepare delta-based climate scenarios of the study area) as presented in the AgMIP (AgMIP, 2013a,b; Ruane et al., 2013). This technique produces climate scenarios for adjusting historically observed weather records at a given site according to changes in precipitation, minimum temperature and maximum temperature predicted by climate model run (Araya et al., 2015). This adjustment is based on predicted absolute changes in temperatures and relative changes in precipitation (Ruane et al., 2013). Future climate projections for both regions were obtained from 20 GCMs for near future (2010–2039), mid (2040–2069) and end (2070–2099) of 21st century under two RCPs (4.5 and 8.5) scenarios using the method developed by AgMIP (AgMIP, 2013a,b). We adopted the corresponding carbon dioxide concentration under RCPs 4.5 and 8.5 for each AgMIP middle year of the three future periods (AgMIP, 2012).

Table 1
Soil physical and chemical characteristics of the experimental locations.

Location	Depth (cm)	Clay (%)	Silt (%)	LL (mm/mm)	DU (mm/mm)	Saturation (mm/mm)	BD (g cm^{-3})	OC (%)	TN (%)
Karaj	0–30	33	37	0.2	0.34	0.44	1.47	0.64	0.08
Khomein	0–30	18	26	0.14	0.31	0.39	1.6	0.4	0.04

LL: lower limit; DU: drained upper limit; BD: bulk density; OC: organic carbon; TN: total nitrogen.

2.5. APSIM-Wheat model calibration and validation

The APSIM-Wheat model was previously calibrated for simulating wheat c. Sivand phenology and grain yield and proved to perform well (R^2 >0.95) for Karaj (Alamoli et al., 2020). Based on their coefficients and to improve parameter accuracy with the nitrogen fertilization treatments, we re-calibrated the APSIM-Wheat model (version 7.5) with data of full irrigation + 200 kg ha^{-1} nitrogen fertilizer (I_1N_1). We obtained the cultivar coefficients step by step, first for phenological development and then for grain developmental parameters. The manual trial and error method was used to determine genetic coefficients (Godwin and Singh, 1998). The values were adjusted to have minimum root mean square error (RMSE), minimum normalized RMSE (%RMSE) (Loague and Green, 1991) and Willmott's index of agreement (IOA) (Willmott et al., 1985), between simulated and observed data. RMSE, % RMSE and IOA were calculated as follows:

$$RMSE = \left[1 \Big/ n \sum_{i=1}^{n} (P_i - O_i)^2\right]^{0.5} \quad (3)$$

$$\%RMSE = \left[1 \Big/ n \sum_{i=1}^{n} (P_i - O_i)^2\right]^{0.5} \times 100 \Big/ \overline{O} \quad (4)$$

$$IOA = 1 - \frac{\sum_{i=1}^{n} (P_i - O_i)^2}{\sum_{i=1}^{n} (|P_i - \overline{P}| + |O_i - \overline{O}|)^2} \quad (5)$$

where O_i refers to the observed biomass and grain yield of wheat, P_i represents predicted wheat biomass and grain yield, $\overline{O}$ is the mean of observed values and $\overline{P}$ is the mean of predicted values. Climate and soil data over time, wheat density and sowing depth, planting time, tillage type and soil preparation time, wheat cultivar, rotation data, irrigation, and harvesting time were all used to simulate wheat phenological stages, LAI development, wheat biomass at harvesting, grain yield, and the harvesting index using data of I_1N_1 (full irrigation and 200 kg ha^{-1} nitrogen) from two locations. We used the module "Plant" for wheat phenology simulations consisting of emergence, end-of-juvenile, floral-initiation, flowering, start-grain-fill, end-grain-fill, maturity, harvest-ripe, end-crop, and the module "SoilWat2" to calculate the content and availability of water at different soil layers taking the various processes such as precipitation, runoff, evaporation, percolation, etc. into account based on the physical characteristics of the soil. Parameters were iterated to minimize absolute mean errors, i.e. differences between predicted and measured output values. The same values of this set of parameters were used in the validation to further evaluate the performance and robustness of APSIM-Wheat. After calibrating the model and validating its performance by comparing with the experimental data, we tested for management options available in APSIM-Wheat such as changing sowing time through the sowing window and irrigation levels to find out their effect in alleviating the drought impacts on wheat production.

3. Results

3.1. Impact of nitrogen fertilization, water deficit and their interactions on wheat performance

Effects of the main factors and their interactions on wheat performance variates are given in Table 2, and comparisons among the treatment means are shown in Table 2 (simple effects) and Fig. 2 (interactions). Averaged over all treatments, a higher wheat biomass was obtained at the Khoemin than the Karaj site, while the grain yield, HI% and LAI was on average higher in Karaj than in Khomein. We also show that I_1 and I_2 had a higher wheat biomasses than I_3 and I_4, while for wheat grain yield, HI% and LAI, I_1, I_2, and I_3 were not significantly different. However, a deficit irrigation over the whole growth period significantly decreased wheat grain yield, HI% and LAI. Increasing nitrogen application (averaged over locations and deficit irrigation treatments) significantly increased wheat biomass, grain yield, HI% and LAI (Table 2).

N_1 had generally the highest wheat biomass, followed by N_2 for both locations except for I_3 in Khomein, where N_2 and N_1 were not significantly different (Fig. 2a). However, with increasing water deficit period the differences between N levels decreased. We observed similar a trend for the wheat grain yield (Fig. 2, b) i.e., $N_1 > N_2 > N_3$ and with increasing water deficit period, a decreasing difference between N levels. Nitrogen application of 50 kg/ha caused the lowest HI% with all irrigation levels (Fig. 2c). However, the difference between N_1 and N_2 was highly dependent on deficit irrigation period and location. With I_1 and I_4 at both sites and with I2 in Karaj, N_1 had higher HI% than N_2, while with I3 at both locations and with I2 in Khomein, N_1 and N_2 statistically differed in HI%. Comparing the LAI values (Fig. 2 d), N_1 produced the highest LAI followed by N_2, except for I_1 in which N_1 and

Table 2
Effect of location, deficit irrigation and nitrogen fertilization on wheat performance and yield. Means with same letter are not significantly different ($P < 0.05$; protected LSD test).

		Wheat biomass (t/ha)	Wheat grain yield (t/ha)		Wheat LAI	Harvesting index (%)
Location	Karaj	9.947 b	4.36 a		3.75 b	43 a
	Khomein	11.28 a	4.13 b		3.9 a	36 b
Irrigation	Full-irrigation	11.50 a	4.77 a		3.91 a	40.9 a
	From grain filling	11.14 a	4.48 a		3.90 a	40 a
	From Flowering	10.27 b	4.14 ab		3.84 a	39.8 a
	Whole-growth	9.53 b	3.60 b		3.6 b	37.7 b
Nitrogen	200 kg/ha	11.94 a	5.62 a		4.3 a	47.1 a
	100 kg/ha	10.31 b	4.13 b		3.9 b	40.2 b
	50 kg/ha	9.59c	2.99c		3.56c	31.5c
Source of variations	df	F-value				
Location	1	167.2 * *	29.79 * *	31.6 * *	600 * *	
Location × Block	6	3.12 *	1.72 ^{ns}	1.2 ^{ns}	1.63 ^{ns}	
Irrigation	3	229.67 * *	10.24 *	11.05 *	13.04 *	
Location × irrigation	3	36.53 * *	31.59 * *	25.2 *	1.83 ^{ns}	
Error	18	0.71 ^{ns}	0.76 ^{ns}	0.89 ^{ns}	1.49 ^{ns}	
Nitrogen	2	384.5 * *	86.33 *	73.4 *	57.22 *	
Location × Nitrogen	2	0.55 ^{ns}	3.38 ^{ns}	0.34 ^{ns}	2.12 ^{ns}	
Irrigation × Nitrogen	6	3.29 ^{ns}	4.93 *	3.5 *	1.63 ^{ns}	
Location × Irrigation ×Nitrogen	6	2.66 *	7.81 * *	6.4 *	12.8 * *	
Error	48					

and * * indicate significance at $P < 0.05$ and $P < 0.01$ levels, respectively.

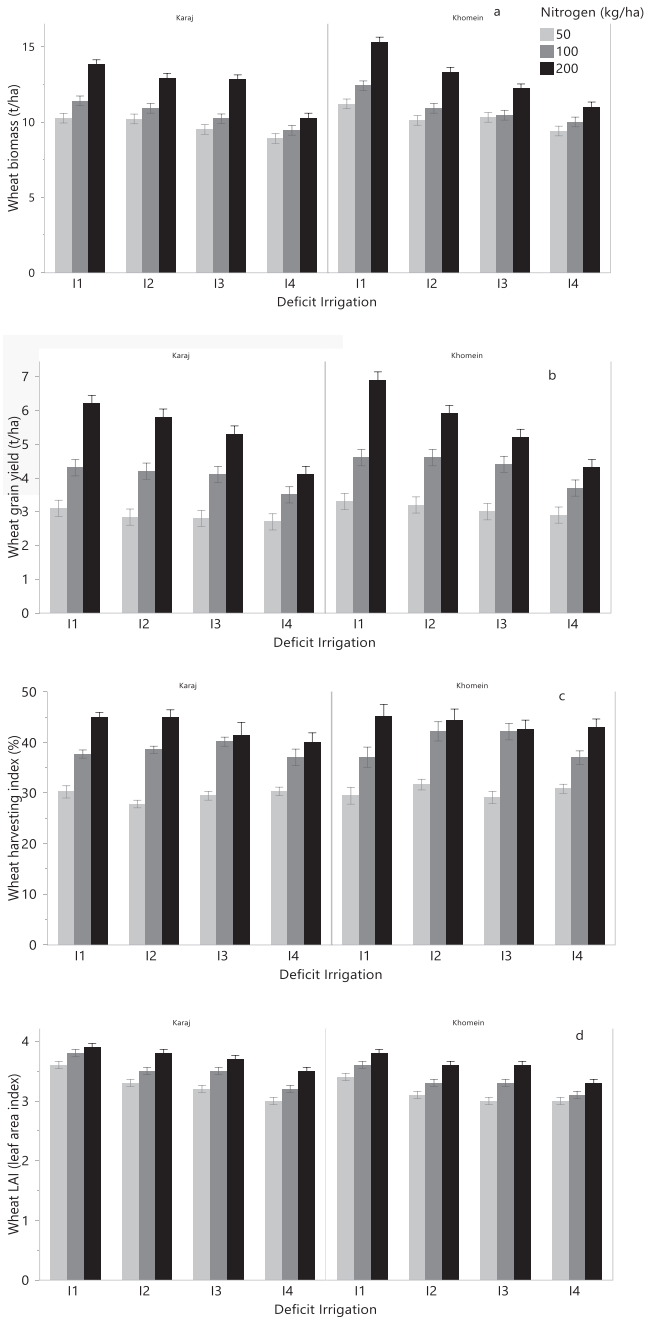

Fig. 2. Treatments means for the two field sites. Error intervals are LSD (least significant difference) values. X axis is the deficit irrigation levels: full irrigation (I_1), deficit irrigation from grain filling ($I_{2,}$), from beginning of flowering (I_2), and during the whole growth period (I_4). Overlapping LSD intervals mean non-significant difference, and non-overlapped intervals mean significant difference.

N_2 and for I_4 in which N_2 and N_3 were not significantly different.

3.2. APSIM-Wheat model calibration and validation

Days to anthesis and maturity at Karaj site were estimated with nRMSE of 4.8 % and 3.2 %, respectively, and at Khomein site with nRMSE of 5.9 % and 2.4 %, respectively. Observed times to anthesis and maturity in Khomein were 14 and 21 days longer than in Karaj, while simulations were 2 and 20 days longer (Table 3). We estimated wheat biomass and grain yield with nRMSE < 3 %, and peak LAI with nRMSE of 9.3 % and 13.3 %, respectively (Table 3). In the following, these

Table 3
Parameterization of APSIM-Wheat model using experimental data of full irrigation + 200 kg ha^{-1} (I_1N_1).

Crop Traits	Karaj			Khomein		
	Obs	Sim	%	Obs	Sim	%
Anthesis (DAP)	104	109	4.8	118	111	5.9
Maturity (DAP)	186	192	3.2	207	212	2.4
mLAI (m^2 m^{-2})	3.84	4.2	9.3	3.89	3.37	13.3
Biomass at harvest (t ha^{-1})	12.87	13.09	1.7	13.59	13.98	2.8
Dry Grain yield (t ha^{-1})	6.96	6.81	2.1	6.09	6.2	1.8

DAP: Days after planting; mLAI: maximum leaf area index.

parameters were used for wheat biomass and grain yield simulation in 11 combinations of irrigation (main plots) × nitrogen (sub-plots) for both locations. With various irrigation × nitrogen treatments, APSIM-Wheat model predicted wheat biomass with RMSE of 0.36–0.7 (t ha^{-1}), nRMSE of 6.6–11.7%, and IOA of 0.88–0.99 at Karaj site, and with RMSE of 0.33–0.58 (t ha^{-1}), nRMSE of 6.1–9.3 %, and IOA of 0.88–0.98 at Khomein site (Table 4). The predictions for the wheat grain yield under varying irrigation regime × nitrogen resulted in RMSE of 0.08–0.6 (t ha^{-1}), nRMSE of 2–11 %, and IOA of 0.89–0.98 for the Karaj site, and of 0.08–0.45 (t ha^{-1}), nRMSE of 2–10.3, and IOA of 0.91–0.96 for the Khomein site (Table 5). Fig. 3 shows the simulation accuracy of APSIM-Wheat for the wheat biomass, LAI, and grain yield. For this, we compared the mean value of each treatment (I_nN_n) as an observation with its corresponding value simulated by APSIM-Wheat. The distribution of data from both sites (as a random effect) around the bisector and low residual deviance implies that the calibrated model performed well.

The simulation of wheat phenology and of the accuracy of the phenological stages are given for both locations in Fig. 4a, b. The R^2 value> 0.99 and RMSE of 3.54 indicate the high performance of the model in simulating wheat phenological stages. For simulating LAI, the model performed well for the Karaj data, but showed some underestimation at peak values for Khomein (Fig. 5a). However, the total performance of the model had a $R^2 > 0.96$ and a RMSE of 0.28 (Fig. 5b).

3.3. Climate change scenarios in the study locations

Regional (for both study locations) precipitation (Pn), evapotranspiration (ETo), maximum (T_{max}) and minimum (T_{min}) temperatures, and Seasonal Precipitation-Evapotranspiration Index (SPEI) under RCP4.5 and RCP8.5 were predicted for the near future (2010–2039), mid-century (2040–2069) and end of century (2070–2099) using 20 GCMs. The period of 1980–2009 was considered as the baseline. The highest and lowest deviance from baseline predicted by 20 GCMs for Pn, Max, Min, ETo, and SPEI are shown in Fig. 6. Simulations for Karaj site suggest that T_{max} and T_{min}, respectively will rise by 1.49 °C and 1.36 °C in 2010–2039, 3.08 °C and 2.69 °C in 2040–2069, and 4.71 °C and 3.93 °C in 2070–2099. For Khomein site, T_{max} and T_{min}, respectively will rise by 0.97 °C and 1.05 °C in 2010–2039, 1.68 °C and 1.79 °C in 2040–2069, and 2.88 °C and 3.02 °C for during 2070–2099.

Seasonal precipitation was simulated to decrease by 1–2% over the three time periods at Karaj site, while at Khomein site, a 3 % increase for 2010–2039, 1 % increase over 2040–2069, and 1 % decrease for 2070–2099 were estimated. ETo will increase by 10–15 % for the Karaj site over three time periods, and for the Khomein site an increase of 4 %, 7 %, and 10 % for 2010–2039, 2040–2069, and 2070–2099, respectively.

3.4. Climate change impact on wheat growth and yield

Fig. 7 shows the various simulations of wheat grain yield for 2010–2039, 2040–2069, and 2070–2099 scenario using different GCMs.

Table 4
Performance of APSIM-Wheat in simulating wheat biomass accumulation (t/ha).

Index	Location	I_1N_2	I_1N_3	I_2N_1	I_2N_2	I_2N_3	I_3N_1	I_3N_2	I_3N_3	I_4N_1	I_4N_2	I_4N_3
RMSE (t ha^{-1})	Karaj	0.47	0.56	0.4	0.43	0.49	0.67	0.7	0.56	0.36	0.53	0.47
	Khomein	0.38	0.5	0.43	0.49	0.58	0.47	0.33	0.41	0.44	0.42	0.54
Normalized RMSE (%)	Karaj	7.7	9.6	7.2	8.2	9.7	10.6	11.7	9.6	6.6	10.4	9.3
	Khomein	5.5	7.7	6.1	7.5	9.3	6.2	4.8	6.2	6.8	6.6	9.2
IOA	Karaj	0.99	0.96	0.99	0.96	0.98	0.94	0.91	0.94	0.96	0.88	0.89
	Khomein	0.98	0.93	0.97	0.94	0.91	0.93	0.97	0.94	0.96	0.93	0.88

I1N2: Full irrigation + 100 kg ha-1 nitrogen; I1N3: Full irrigation + 50 kg ha-1 nitrogen; I2N1: Deficit irrigation from grain filling + 200 kg ha-1 nitrogen; I2N2: Deficit irrigation from grain filling + 100 kg ha-1 nitrogen; I2N3: Deficit irrigation from grain filling + 50 kg ha-1 nitrogen; I3N1: Deficit irrigation from the beginning of flowering + 200 kg ha-1 nitrogen; I3N2: Deficit irrigation from the beginning of flowering + 100 kg ha-1 nitrogen; I3N3: Deficit irrigation from the beginning of flowering + 50 kg ha-1 nitrogen; I4N1: Deficit irrigation in whole period of crop growth + 200 kg ha-1 nitrogen; I4N2: Deficit irrigation in whole period of crop growth + 100 kg ha-1 nitrogen; I4N3: Deficit irrigation in whole period of crop growth + 50 kg ha-1 nitrogen.

Table 5
Performance of APSIM-Wheat in simulating wheat grain yield (t ha^{-1}).

index	Region	I_1N_2	I_1N_3	I_2N_1	I_2N_2	I_2N_3	I_3N_1	I_3N_2	I_3N_3	I_4N_1	I_4N_2	I_4N_3
RMSE (t ha^{-1})	Karaj	0.24	0.21	0.04	0.04	0.06	0.36	0.37	0.1	0.2	0.23	0.08
	Khomein	0.08	0.18	0.45	0.19	0.18	0.37	0.28	0.21	0.25	0.27	0.24
Normalized RMSE (%)	Karaj	9	9.2	1.8	2	2.9	11	14.3	4.6	8	10.9	4.2
	Khomein	2	7.5	10	5.3	7.4	7.7	7.2	8.7	6.4	8.5	10.3
IOA	Karaj	0.97	0.95	0.98	0.97	0.96	0.89	0.91	0.96	0.94	0.9	0.96
	Khomein	0.96	0.95	0.91	0.94	0.93	0.91	0.93	0.95	0.93	0.96	0.92

abbreviations as in Table 3.

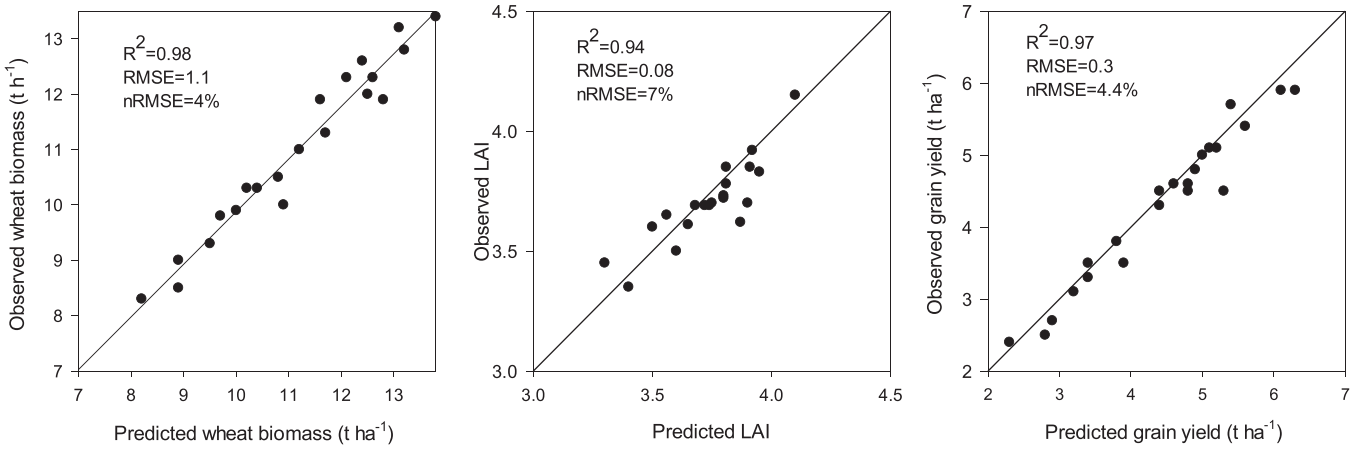

Fig. 3. Simulated wheat biomass, leaf area index (LAI), and grain yield by APSIM-Wheat compared to the observed experimental data.

At Karaj site (Fig. 7a), simulating 2010–2039 with all GCMs except for ACCSEEI-0 (with RCP4.5) and HadGEM2-ES (with RCP8.5), wheat grain yield is expected to increase. For mid and end-century periods, all GCMs simulate decreasing wheat grain yield, however, more severe with RCP8.5 and for the 2070–2099 period.

At Khomein site (Fig. 7b) over 2010–2039, some rare GCMs simulate a little decrease, but most GCMs simulate increases in wheat grain yield. For 2040–2069, with RCP4.5, except of two GCMs that simulate little decreases, all other GCMs simulate an increasing wheat grain yield. With RCP8.5, although most GCMs simulate decreasing grain yield, two models simulate an increase of wheat yield. For 2070–2099, both RCP4.5 and 8.5 simulate a decreasing wheat grain yield, being more severe by the latter one.

Table 6 shows the simulated wheat grain yield and growing season length with varying CO_2 over RCP 4.5 and 8.5. For 2010–2039, with RCP4.5, growing season length may decrease by 1 % and 2 % at the Karaj and Khomein site, respectively, and wheat grain yield is estimated to increase by 2 % for both locations; with RCP8.5, growing season length is estimated to experience the same decrease, while grain yield is simulated to increase by 3 % for both locations.

During 2040–2069 and with RCP4.5, we simulate an 8 % decrease in growing season and a 7 % decrease in grain yield at the Karaj site. At the Khomein site, we simulate a 4 % increase of wheat grain yield and a 4 % decrease of growing season length. Assuming RCP 8.5, the model suggests a 10 % and 14 % decrease of the growing season length for Karaj and Khomein, respectively, and a 9 % and a 4 % decrease in wheat grain yield for the respective sites.

Simulations of RCP4.5 for 2070–2099 suggest 11 % and 15 % decreases of growing season length in Karaj and Khomein, respectively, and accordingly a 16 % and 14 % decrease in wheat grain yield at Karaj and Khomein, respectively. The decrease in growing season length and grain yield is predicted to be greater with RCP8.5 for both sites.

4. Discussion

We acknowledge that our study only used one year of data for calibration and validation besides the high number of experimental plots. Nevertheless, we are confident with the accuracy of the model outcomes. First, we used formerly estimated model coefficients, and then initiated re-calibration for interactive effects between nitrogen levels

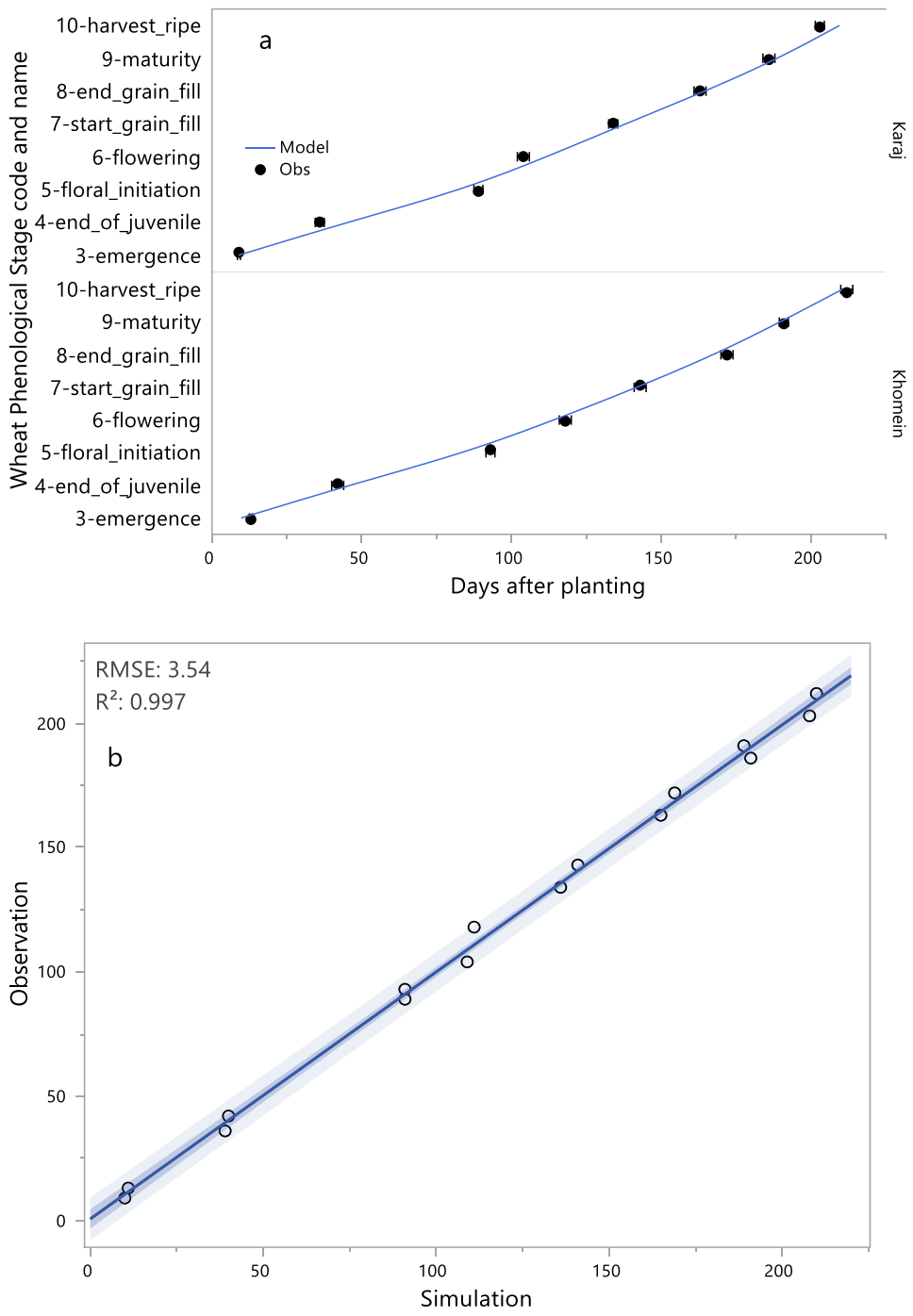

Fig. 4. Observed (markers) and simulated phenological stages of wheat at two locations (a). Simulated phenological stages of wheat compared to the observed experimental data (b).

and drought periods. Secondly, the locations selected for the study were chosen to capture meaningful differences in climates, and finally, the total performance of the model had a R2 > 0.96 and a RMSE of 0.28 (Fig. 5b).

4.1. GCMs simulations: Do variations matter

Our scenarios suggest an overall decline in precipitation and increases in T_{max} and T_{min} but we also found inconsistencies in simulating climate among GCMs. There were ranges of standard deviation (sd) for predicting precipitation (sd=10.8–28.8), ET_o (sd=3.17–10.81), T_{max} (sd= 0.16–0.56), T_{min} (sd=0.18–0.59), and EPSI (sd= 0.01–0.04) (Fig. 6). Previous climate projections have shown a decline in precipitation and increase in T_{max} and T_{min}, however the use of multi-GCMs and multi-emission scenarios was highly recommended to improve bias and uncertainty in future climate projection (Chen et al., 2010; Zhang et al., 2011; Turco et al., 2013).

Model discrepancies arise from many sources, such as structural uncertainty caused by representing the atmosphere by a finite number of variables, uncertainties in physical and sub grid-scale parameterization schemes, and uncertainty in how best to choose the model parameters (Ho et al., 2012). Uncertainties are greater with interactive increased temperature and elevated CO_2 (Cammarano et al., 2016), and depend on different spatial and time scale averages. In general, uncertainty of

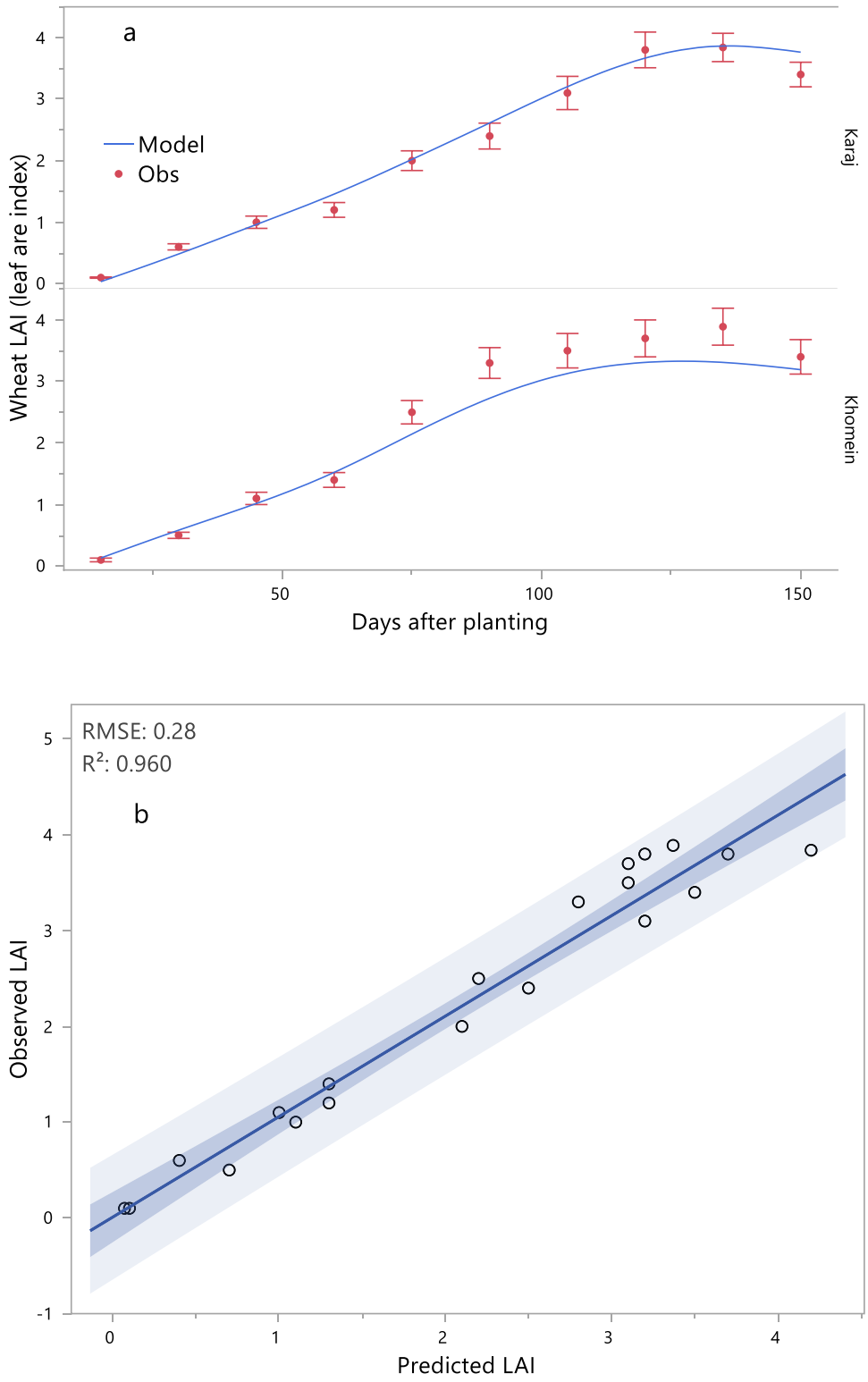

Fig. 5. Observed (markers) and simulated LAI development of wheat at two locations (a). Simulated LAI development of wheat compared to the observed experimental data (b).

internal variables becomes more important on shorter time scales and for smaller scale variables (Giorgi, 2010).

4.2. *Impacts on the length of the wheat growing season and on yield*

The error% in anthesis prediction was 4–6 % but for maturity less than 3%. Sivand is an Iranian wheat cultivar, an early type spring variety with 90 cm height, known to show significant phenotypic plasticity in phenological growth and yield under different environments (Najafian et al., 2010). The range of plasticity in wheat was reported to be 0.74–1.27 for yield and 0.85–1.17 for time to anthesis. The duration of the post-anthesis period as a fraction of the season was the trait with the largest range of plasticity, i.e., 0.47–1.80 (Sadras et al., 2009). Anthesis time prediction has been a challenge that shows inconsistency over

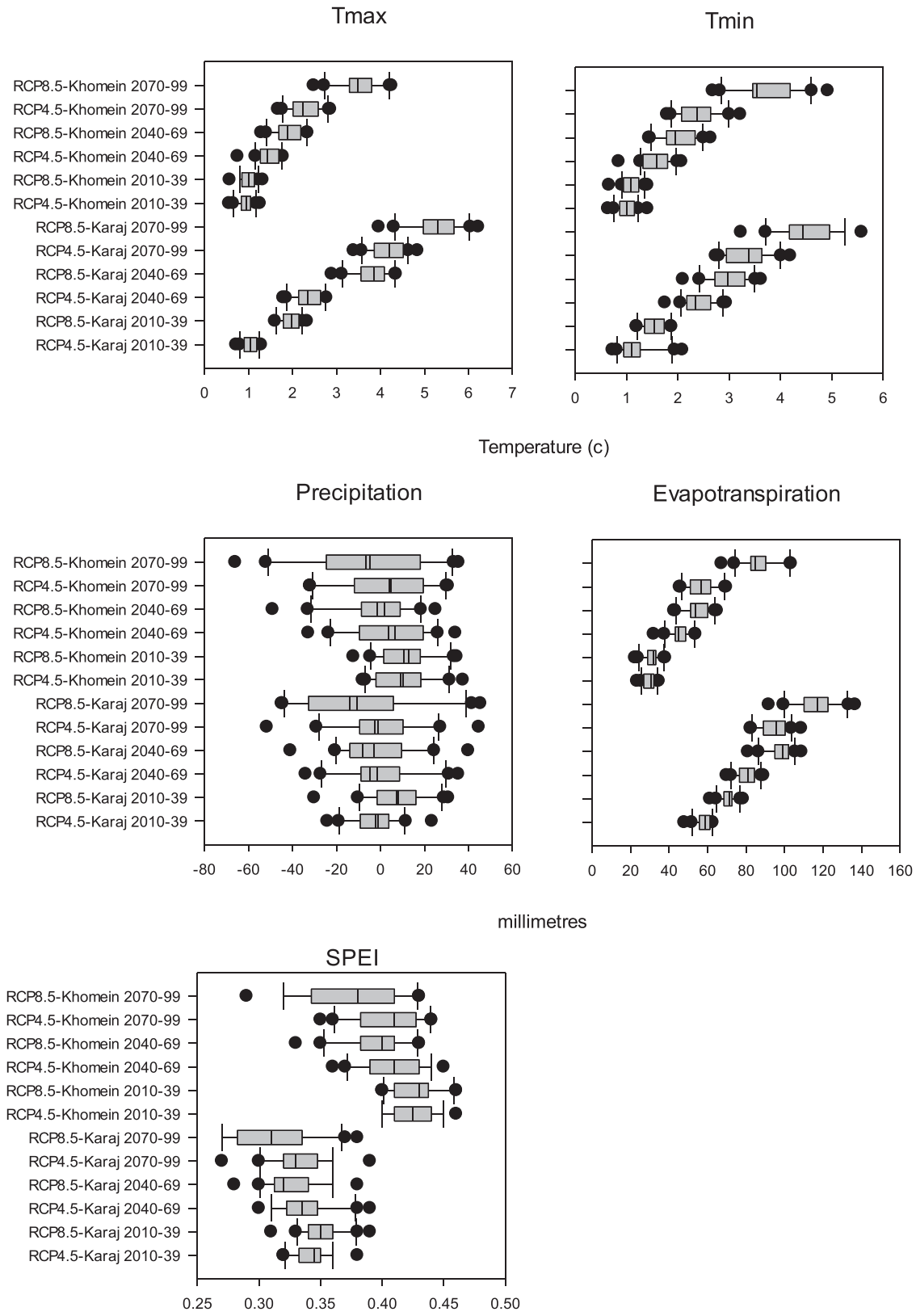

Fig. 6. Boxplots for predicted maximum temperatures (T_{max}), minimum temperatures (T_{min}), precipitation, evapotranspiration, and Seasonal Precipitation-Evapotranspiration Index (SPEI) using 20 GCMm for 2010–2039, 2040–2069, 2070–2099 with RCP4.5 and RCP8.5.

different environments (Lamsal et al., 2018). However, our model gave a good prediction of the maturity time and accordingly yield.

Models simulate future warmer conditions for wheat growth, and higher temperature leading to a shortened growing season and lower wheat yield. However, the decrease of wheat yield with rising temperature is predicted to be different between locations (Fig. 8). For Karaj, the decrease in grain yield is predicted to be linear, while logistic for Khomein. Locations with lower average temperature and higher

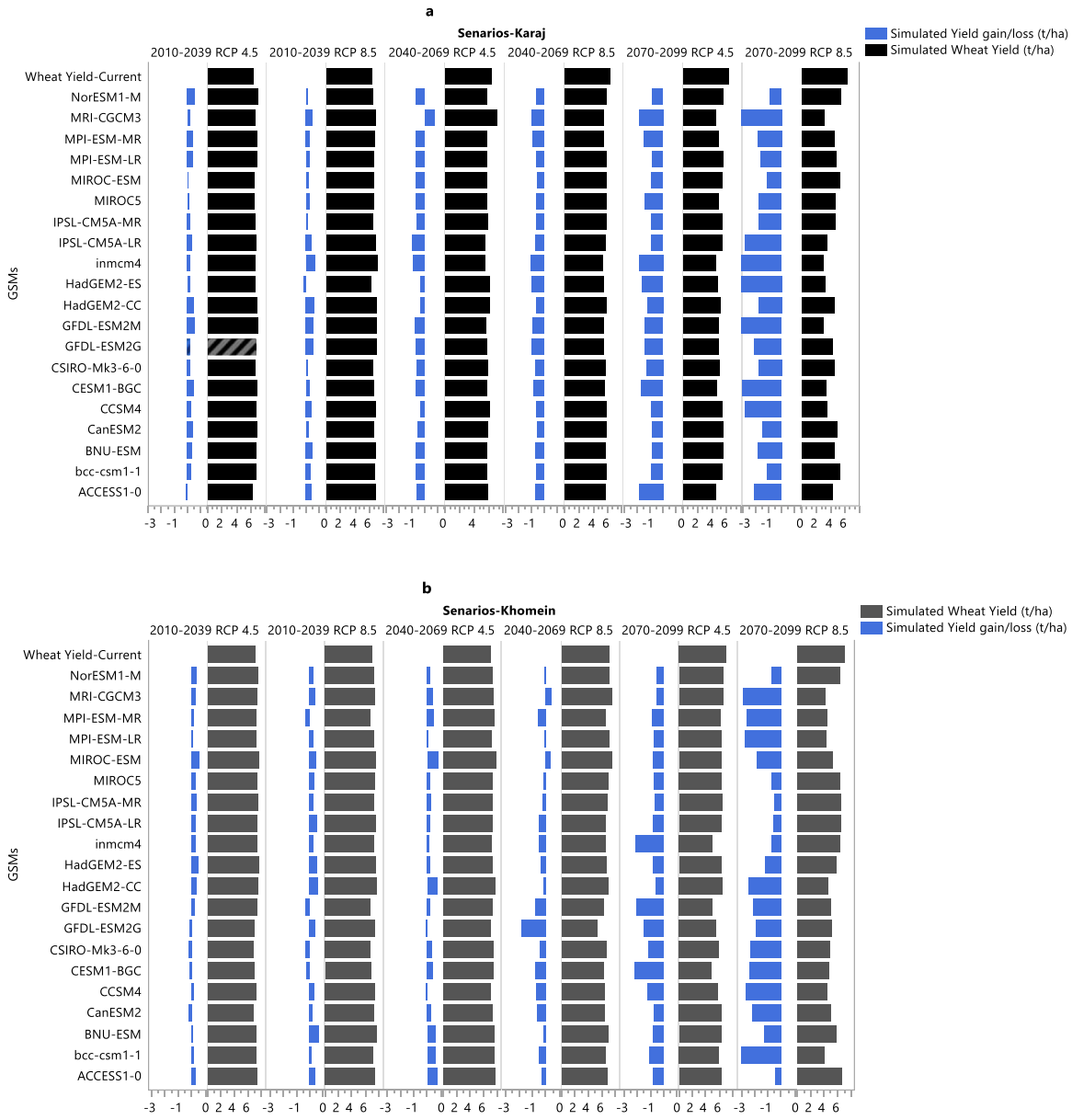

Fig. 7. Wheat yield (black bars) and yield gained/lost (as compared to the historical average, blue bars) simulated by APSIM-Wheat based on 20 GCM under RCP4.5 and RCP8.5 for 2010–2039, 2040–2069, and 2070–2099 in Karaj and Khomein.

Table 6
Change of yield and growing season length over three future time periods simulated by APSIM model based on 20 GCMs with RCP4.5 and RCP8.5.

Time period	RCP	Assumed average CO2 concentration for the period (ppm)	Median yield change based on 20 GCM (%)		Median growth duration change based on 20 GCM (%)	
			Karaj	Khomein	Karaj	Khomein
2010–2039	RCP4.5	423	2	2	-1	-2
2010–2039	RCP8.5	432	3	3	-1	-2
2040–2069	RCP4.5	499	-7	4	-8	-4
2040–2069	RCP8.5	571	-9	-4	-10	-14
2070–2099	RCP4.5	532	-16	-14	-11	-15
2070–2099	RCP8.5	801	-31	-20	-16	-21

precipitation can better resist against rising temperature impact, therefore a 1–2 centigrade increase does not lead to a decrease in yield (Roshan et al., 2014). Luo and Kathuria (2013) suggested that in locations that suffer from drought, the growing season length will be shorter due to temperature increase. Fig. 1 shows that Karaj has a higher temperature and a longer period of hot days, and accordingly higher ETo rates. Moreover, Khomein not only has a higher precipitation, but rainfalls are more homogenously over the days of the year. Therefore, this site can benefit from one centigrade increase of temperature.

Our simulation models revealed a positive effect of enhanced CO_2 on wheat yield over 2010–2039 for both locations, and over 2040–2069 at Khomein site with RCP 4.5 (Table 6). If not encountering severe

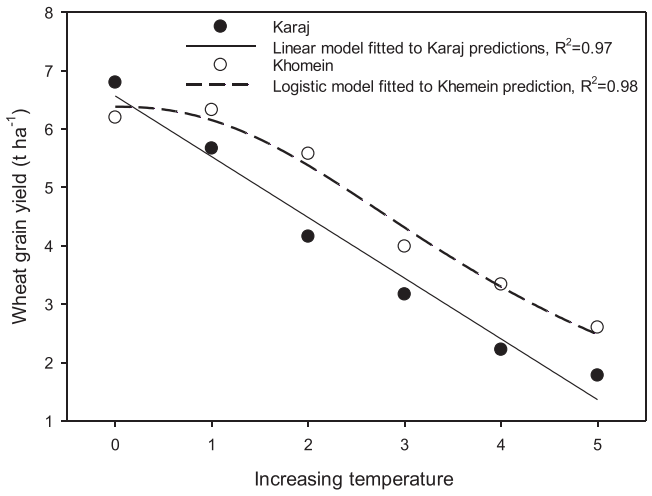

Fig. 8. Increasing temperature decreases wheat grain yield. The decreasing trend is linear for the Karaj site, while logistic for the Khomein site.

drought, increasing CO_2 can mitigate negative impacts of temperature and of a shorter growing season. Wang et al. (2009) suggested that doubling CO_2 from 350 ppm to 700 ppm increased wheat yield by 36 %. Increasing CO_2 can increase yields in C_3 crops such as wheat via improved water use efficiency. Through our simulations, we found a small decreasing impact of temperature with elevated CO_2 at both sites (Fig. 9). The model simulates that with high CO_2 rates, the temperature impact may act reversely causing some increase in wheat grain yield. Driever et al. (2017) showed that elevated CO_2 mitigated heat stress impact on wheat yield. Duan et al. (2018) also suggested that the elevated CO_2 decreased the temperature impact. Furthermore, as shown by Broberg et al. (2019), an elevated CO_2 effect is highly dependent on site productivity such as soil nutrients. In a chamber experiment, de Oliveira et al. (2013) showed that elevated CO_2 can alleviate temperature impact on wheat, but there are also inconsistent results showing that increasing CO_2 is unable to compensate for the impact of temperature increase in wheat and rice (Cai et al., 2016). Chavan et al. (2019) showed that CO_2 mitigated the negative impacts of heat stress at anthesis on wheat photosynthesis and biomass, and that grain yield was reduced by heat stress in both CO_2 treatments. Mitchel et al. (1999) showed that elevated CO_2 did not increase grain yield and did not decrease the negative impact of higher temperature in the field.

4.3. Management options to adapt to climate change impacts

4.3.1. Nitrogen fertilization

We showed that nitrogen application could reduce the drought impact on wheat performance traits. Supplementing nutrient is an approach to reduce the impacts of water stress on growth and productivity of crops. Exposure to drought is known be more detrimental at the vegetative than reproductive stage, and nitrogen application via regulating physiological and biochemical mechanisms could improve drought tolerance in plant (Hussain et al., 2016). Adequate N application could enhance root proliferation under drought and thus alleviate drought tolerance (Song et al., 2019). Sedri et al. (2022) and Shabbir et al. (2016) specifically showed that N application could improve the tolerance of wheat cultivar to drought stress.

4.3.2. Compensative irrigation

Evaluating the effect of irrigation on wheat yield under five levels of temperature increase (1–5 °C) suggests that at the Karaj site, yield loss could be reduced by 12.6 % and 24.7 % with increasing irrigation water by 30 % (on average 9 mm/day) and 40% (on average c. 10 mm/day) above the conventional irrigation, respectively. More specifically, Heng et al. (2007) showed that a small irrigation amount at sowing could have a large effect on yield. Birthal et al. (2021) highlighted that heat stress negatively impacts crop yield, and its impact has increased over the past 60 year. Irrigation moderates the harmful impact of heat stress, but over time its effectiveness has declined. With increasing shortage of irrigation water and rising temperature, technological and policy options need to be explored for improving irrigation water-use efficiency and breeding of crops for heat tolerance and low water footprints.

Our simulation study highlights that conventional (8 mm per day) and excessive irrigation (9 mm per day) decrease yield losses to 8.28 % and 3.34 %, respectively at the Khomein site. Wang et al. (2009), reported that each 60 mm additional irrigation would lead to an increase in yield by 1.2 t ha^{-1}, and that 540 mm irrigation increased wheat yield to 7.1 t ha^{-1}. However, as the water supply is short in arid region, excessive irrigation is not an option.

4.3.3. Earlier sowing

Our simulation study showed for the Karaj site and under five levels of temperature increase (1–5 °C) a grain yield loss with the conventional

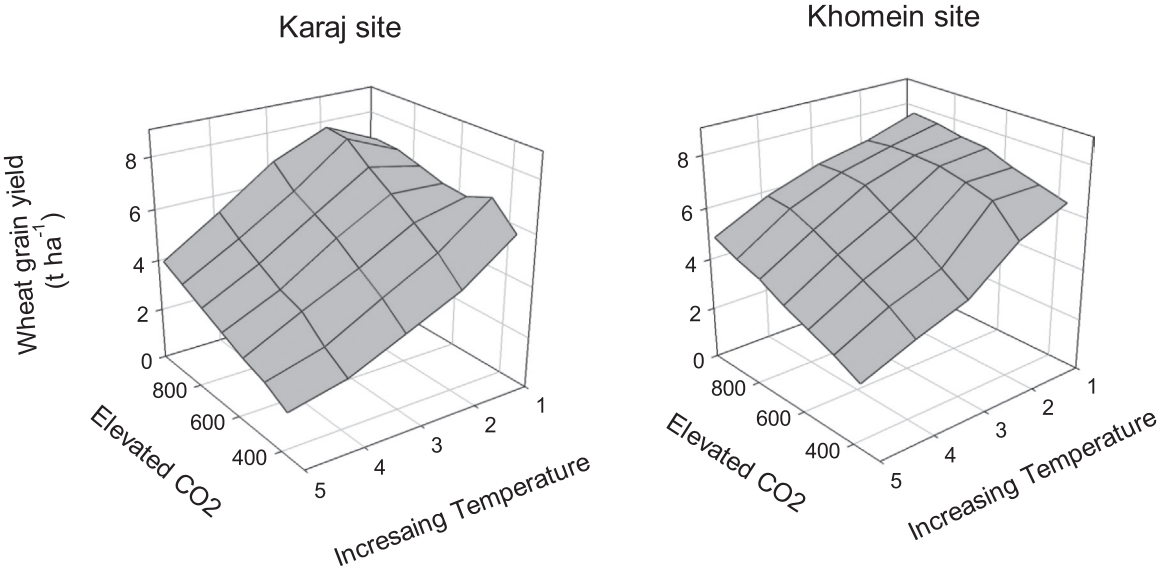

Fig. 9. Wheat grain yield as affected by increasing temperature and elevated CO_2 in Karaj and Khomein.

sowing date (11th November) of 24.67 %, but only 8.76 %, i.e., 16 % lower yield loss with an earlier sowing date (12th October). For the Khomein site, the conventional sowing date (31st October) resulted in 8.14 % yield loss, while early sowing (1st October) simulates only 0.9 % yield loss. This clearly indicates that early sowing can alleviate the risk of yield loss under high temperature during flowering and grain filling periods, thus constituting an effective adaptation strategy in dealing with climate change impact. Furthermore, using early and tolerant varieties have also been proposed to adapt to climate change effects (Hernandez-Ochoa et al., 2019).

5. Conclusions

Using the field experimental data, our simulation study showed that climate change impacts by increasing temperature and drought could decrease wheat yield in the longer term, while a marginal increase in wheat yield may occur in the short-term (2010–2039). For 2040–2069 and 2070–2099 scenarios, most models simulate a decreased growing season length and accordingly decreased wheat yield. We also simulated a positive effect of elevated CO_2 on wheat yield over near- to mid-future if not encountering severe drought. Irrigation at an excessive rate can alleviate the negative climate change impact. However, in countries such as Iran that are suffering from serious drought, excessive irrigation is not an option. Our study highlights that earlier sowing dates combined with adequate fertilization should be considered to adapt to climate change impacts on crop yield in areas where excess in irrigation water is not available.

CRediT authorship contribution statement

Hossein Moghaddam: Method, Writing—Original Draft Preparation, Supervision;**Mostafa Oveisi:** Conceptualization, Validation, Formal Analysis, Writing—Original Draft. Preparation, Writing—Review and Editing, Visualization, Supervision;**Mostafa Keshavarz Mehr:** Software, Investigation, Writing—Original Draft Preparation;**Javad Bazrafshan:** Method, Supervision;**Mohammad Hossein Naeimi:** Writing—Original Draft Preparation, Writing—Review and Editing;**Behnaz Pourmorad Kaleibar:** Writing—Original Draft Preparation, Writing—Review and Editing;**Heinz Müller-Schärer:** Conceptualization, Writing—Original Draft Preparation, Writing—Review. and Editing, Supervision, Funding Acquisition.

Declaration of Competing Interest

The authors declare no conflict of interest.

Data availability

No data was used for the research described in the article.

Acknowledgment

This study was partially supported by the Swiss National Science Foundation (project number 31003A_166448 to H. Müller-Schärer).

References

AgMIP, 2013b. The coordinated climate-crop modeling project c3mp: An initiative of the agricultural model intercomparison and improvement project. C3MP Protoc. Proced. ⟨http://research.agmip.org/download/attachments/1998899/C3MP+Protocols+v2.pdf/⟩.

Alamoli, Z.R., Jahansouz, M., Hosseini, S.M.B., Soufizadeh, S., 2020. Evaluation the growth characteristics, yield and yield components of wheat and barley under water and nitrogen stress conditions. Iran. J. Field Crop Sci. 51 (2), 87–104. https://doi.org/10.22059/ijfcs.2019.264529.654518.

Araya, A., Hoogenboom, G., Luedeling, E., Hadgu, K.M., Kisekka, I., Martorano, L.G., 2015. Assessment of maize growth and yield using crop models under present and future climate in southwestern Ethiopia. Agric. For. Meteorol. 214, 252–265. https://doi.org/10.1016/j.agrformet.2015.08.259.

Barros, V.R., Boninsegna, J.A., Camilloni, I.A., Chidiak, M., Magrín, G.O., Rusticucci, M., 2015. Climate change in Argentina: trends, projections, impacts and adaptation. Wiley Interdiscip. Rev.: Clim. Change 6 (2), 151–169. https://doi.org/10.1002/wcc.316.

Chavan, S.G., Duursma, R.A., Tausz, M., Ghannoum, O., 2019. Elevated CO_2 alleviates the negative impact of heat stress on wheat physiology but not on grain yield. J. Exp. Bot. 70 (21), 6447–6459. https://doi.org/10.1093/jxb/erz386.

de Mendiburu, F. and de Mendiburu, M.F., 2019. Package 'agricolae'. R Package, version, 1(3).

Driever, S.M., Simkin, A.J., Alotaibi, S., Fisk, S.J., Madgwick, P.J., Sparks, C.A., Raines, C.A., 2017. Increased SBPase activity improves photosynthesis and grain yield in wheat grown in greenhouse conditions. Philos. Trans. R. Soc. B: Biol. Sci. 372 (1730), 20160384. https://doi.org/10.1098/rstb.2016.0384.

Duan, H., Chaszar, B., Lewis, J.D., Smith, R.A., Huxman, T.E., Tissue, D.T., 2018. CO_2 and temperature effects on morphological and physiological traits affecting risk of drought-induced mortality. Tree Physiol. 38 (8), 1138–1151. https://doi.org/10.1093/treephys/tpy037.

Giorgi, F., 2010. Uncertainties in climate change projections, from the global to the regional scale. EPJ Web Conf. 9, 115–129. https://doi.org/10.1051/epjconf/201009009.

Godwin, D.C., Singh, U., 1998. Nitrogen balance and crop response to nitrogen in upland and lowland cropping systems. Understanding Options for Agricultural Production. Springer,, Dordrecht, pp. 55–77. https://doi.org/10.1007/978-94-017-3624-4_4.

Hargreaves, G.H., Samani, Z.A., 1985. Reference crop evapotranspiration from temperature. Appl. Eng. Agric. 1 (2), 96–99. https://doi.org/10.13031/2013.26773.

Heng, L.K., Asseng, S., Mejahed, K., Rusan, M., 2007. Optimizing wheat productivity in two rain-fed environments of the West Asia–North Africa region using a simulation model. Eur. J. Agron. 26 (2), 121–129. https://doi.org/10.1016/j.eja.2006.09.001.

Hernandez-Ochoa, I.M., Pequeno, D.N.L., Reynolds, M., Babar, M.A., Sonder, K., Milan, A.M., Hoogenboom, G., Robertson, R., Gerber, S., Rowland, D.L., Fraisse, C. W., 2019. Adapting irrigated and rainfed wheat to climate change in semi-arid environments: management, breeding options and land use change. Eur. J. Agron. 109, 125915 https://doi.org/10.1016/j.eja.2019.125915.

Ho, C.K., Stephenson, D.B., Collins, M., Ferro, C.A.T., Brown, S.J., 2012. Calibration strategies: a source of additional uncertainty in climate change projections. Bull. Am. Meteorol. Soc. 93 (1), 21–26. ⟨http://www.jstor.org/stable/26218622⟩.

Hussain, R.A., Ahmad, R., Nawaz, F., Ashraf, M.Y., Waraich, E.A., 2016. Foliar NK application mitigates drought effects in sunflower (*Helianthus annuus* L.). Acta Physiol. Plant. 38, 1–14. https://doi.org/10.1007/s11738-016-2104-z.

Jamali, M.R., Baghestani, M.A., Jokar, L., 2017. Control of wild barley by sulfosulfuron+met sulfuron (Total) and sulfosulfuron (Apyrus) herbicides using time of application and wheat density. Iran. J. Field Crop Sci. 47 (3), 393–400 magiran.com/p163392).

Khosravi, H., Zehtabian, G., Ahmadi, H., Azarnivand, H., 2014. Hazard assessment of desertification as a result of soil and water recourse degradation in Kashan Region, Iran. Desert 19 (1), 45–55. https://doi.org/10.22059/JDESERT.2014.51053.

Korres, N.E., Norsworthy, J.K., Tehranchian, P., Gitsopoulos, T.K., Loka, D.A., Oosterhuis, D.M., Gealy, D.R., Moss, S.R., Burgos, N.R., Miller, M.R., Palhano, M., 2016. Cultivars to face climate change effects on crops and weeds: a review. Agron. Sustain. Dev. 36 (1), 1–22. https://doi.org/10.1007/s13593-016-0350-5.

Lamsal, A., Welch, S.M., White, J.W., Thorp, K.R., Bello, N.M., 2018. Estimating parametric phenotypes that determine anthesis date in Zea mays: challenges in combining ecophysiological models with genetics. PLOS One 13 (4), e0195841. https://doi.org/10.1371/journal.pone.0195841.

Lange, M.A., 2019. Impacts of climate change on the eastern Mediterranean and the Middle East and North Africa region and the water–energy nexus. Atmosphere 10 (8), 455. https://doi.org/10.3390/atmos10080455.

Loague, K., Green, R.E., 1991. Statistical and graphical methods for evaluating solute transport models: overview and application. J. Contam. Hydrol. 7 (1–2), 51–73. https://doi.org/10.1016/0169-7722(91)90038-3.

López-Urrea, R., Montoro, A., González-Piqueras, J., López-Fuster, P., Fereres, E., 2009. Water use of spring wheat to raise water productivity. Agric. Water Manag. 96 (9), 1305–1310.

Ministry of Agriculture-Jahad, 2014. Agric. Stat. 1, 2013–2014. ⟨http://www.maj.ir/Portal/Home/.pdf⟩.

Ministry of Agriculture-Jahad, 2019. Agric. Stat. 1, 2017–2018. ⟨https://www.maj.ir/Dorsapax/userfiles/Sub65/Amarnamehj1-96-97-site.pdf⟩.

AgMIP, 2013a. Guide for running AgMIP climate scenario generation tools with R in windows. ⟨http://www.agmip.org/wp-content/uploads/2013/10/Guide-for-Running-AgMIP-Climate-Scenario-Generation-with-R-v2.3.pdf/⟩.

, 2012AgMIP. 2012. Guide for regional integrated assessments: Handbook of methods and procedures, version 4.2. http://www.agmip.org/wp-content/uploads/2013/06/AgMIP-Regional-Research-Team-Handbook-v4.2.pdf/.

Akbari, M., Neamatollahi, E., Neamatollahi, P., 2019. Evaluating land suitability for spatial planning in arid regions of eastern Iran using fuzzy logic and multi-criteria analysis. Ecol. Indic. 98, 587–598. https://doi.org/10.1016/j.ecolind.2018.11.035.

Asseng, S., Ewert, F., Martre, P., Rötter, R.P., Lobell, D.B., Cammarano, D., Reynolds, M. P., 2015. Rising temperatures reduce global wheat production. Nat. Clim. Change 5 (2), 143–147. https://doi.org/10.1038/NCLIMATE2470.

Birthal, P.S., Hazrana, J., Negi, D.S., Pandey, G., 2021. Benefits of irrigation against heat stress in agriculture: evidence from wheat crop in India. Agric. Water Manag. 255, 106950 https://doi.org/10.1016/j.agwat.2021.106950.

Broberg, M.C., Högy, P., Feng, Z., Pleijel, H., 2019. Effects of elevated CO_2 on wheat yield: non-linear response and relation to site productivity. Agronomy 9 (5), 243. https://doi.org/10.3390/agronomy9050243.

Cai, C., Yin, X., He, S., Jiang, W., Si, C., Struik, P.C., Pan, G., 2016. Responses of wheat and rice to factorial combinations of ambient and elevated CO_2 and temperature in FACE experiments. Glob. Change Biol. 22 (2), 856–874. https://doi.org/10.1111/gcb.13065.

Cammarano, D., Rötter, R.P., Asseng, S., Ewert, F., Wallach, D., Martre, P., Boote, K.J., 2016. Uncertainty of wheat water use: simulated patterns and sensitivity to temperature and CO_2. Field Crops Res. 198, 80–92. https://doi.org/10.1016/j.fcr.2016.08.015.

Chen, H., Guo, J., Xiong, W., Guo, S., Xu, C.Y., 2010. Downscaling GCMs using the smooth support vector machine method to predict daily precipitation in the Hanjiang basin. Adv. Atmos. Sci. 27 (2), 274–284. https://doi.org/10.1007/s00376-009-8071-1.

, 2018FAO: Food and agriculture organization, 2018. Arid zone forestry: A guide for field technicians. http://www.fao.org/docrep/t0122e/t0122e00.htm#Contents.

Luo, Q., Kathuria, A., 2013. Modelling the response of wheat grain yield to climate change: a sensitivity analysis. Theor. Appl. Climatol. 111 (1–2), 173–182. https://doi.org/10.1007/s00704-012-0655-5.

Montesino-San Martín, M., Olesen, J.E., Porter, J.R., 2014. A genotype, environment and management (GxExM) analysis of adaptation in winter wheat to climate change in Denmark. Agric. For. Meteorol. 187, 1–13. https://doi.org/10.1016/j.agrformet.2013.11.009.

Najafi, M.R., Moradkhani, H., 2015. Multi-model ensemble analysis of runoff extremes for climate change impact assessments. J. Hydrol. 525, 352–361. https://doi.org/10.1016/j.jhydrol.2015.03.045.

Najafian, G., Amin, H., Afshari, F., Pazhomand, M.E., Dadaeen, M., Zakeri, A., Yasaie, M., Rajaie, S., Nikzad, A.R., Nikooseresht, R. and Ghandi, A., 2010. Sivand, a new bread wheat cultivar, resistant to stem rust (race Ug99) with good bread making quality for cultivation under irrigated conditions of temperate regions of Iran. https://www.sid.ir/paper/147063/en.

de Oliveira, E.D., Bramley, H., Siddique, K.H., Henty, S., Berger, J., Palta, J.A., 2013. Can elevated CO_2 combined with high temperature ameliorate the effect of terminal drought in wheat? Funct. Plant Biol. 40 (2), 160–171. https://doi.org/10.1071/FP12206.

Pachauri, R.K., Allen, M.R., Barros, V.R., Broome, J., Cramer, W., Christ, R.,. & Dubash, N.K., 2014. Climate change 2014: synthesis report. Contribution of Working Groups I, II and III to the fifth assessment report of the Intergovernmental Panel on Climate Change (p. 151). Ipcc. https://hdl.handle.net/10013/epic.45156.

Pirttioja, N., Carter, T.R., Fronzek, S., Bindi, M., Hoffmann, H., Palosuo, T., Asseng, S., 2015. Temperature and precipitation effects on wheat yield across a European transect: a crop model ensemble analysis using impact response surfaces. Clim. Res. 65, 87–105. https://doi.org/10.3354/cr01322.

Roshan, G., Oji, R., Al-Yahyai, S., 2014. Impact of climate change on the wheat-growing season over Iran. Arab. J. Geosci. 7 (8), 3217–3226. https://doi.org/10.1007/s12517-013-0917-2.

Ruane, A.C., Cecil, L.D., Horton, R.M., Gordón, R., McCollum, R., Brown, D., Rosenzweig, C., 2013. Climate change impact uncertainties for maize in Panama: farm information, climate projections, and yield sensitivities. Agric. For. Meteorol. 170, 132–145. https://doi.org/10.1016/j.agrformet.2011.10.015.

Ruane, A.C., Goldberg, R., Chryssanthacopoulos, J., 2015. Climate forcing datasets for agricultural modeling: Merged products for gap-filling and historical climate series estimation. Agric. For. Meteorol. 200, 233–248. https://doi.org/10.1016/j.agrformet.2014.09.016.

Sadras, V.O., Reynolds, M.P., De la Vega, A.J., Petrie, P.R., Robinson, R., 2009. Phenotypic plasticity of yield and phenology in wheat, sunflower and grapevine. Field Crops Res. 110 (3), 242–250. https://doi.org/10.1016/j.fcr.2022.108583.

Scherer, T.F., and Steele, D.D., 2019. Irrigation scheduling by the checkbook method. library.ndsu.edu.

Sedri, M.H., Roohi, E., Niazian, M., Niedbała, G., 2022. Interactive effects of nitrogen and potassium fertilizers on quantitative-qualitative traits and drought tolerance indices of rainfed wheat cultivar. Agronomy 12, 1–30. https://doi.org/10.3390/agronomy12010030.

Shabbir, R.N., Waraich, E.A., Ali, H., Nawaz, F., Ashraf, M.Y., Ahmad, R., Awan, M.I., Ahmad, S., Irfan, M., Hussain, S., Ahmad, Z., 2016. Supplemental exogenous NPK application alters biochemical processes to improve yield and drought tolerance in wheat (*Triticum aestivum* L.). Environ. Sci. Pollut. Res. 23, 2651–2662. https://doi.org/10.1007/s11356-015-5452-0.

Shi, W., Tao, F., Zhang, Z., 2013. A review on statistical models for identifying climate contributions to crop yields. J. Geogr. Sci. 23 (3), 567–576. https://doi.org/10.1007/s11442-013-1029-3.

Song, J., Wang, Y., Pan, Y., Pang, J., Zhang, X., Fan, J., Zhang, Y., 2019. The influence of nitrogen availability on anatomical and physiological responses of Populus alba× P. glandulosa to drought stress. BMC Plant Biol. 19, 1–12. https://doi.org/10.1186/s12870-019-1667-4.

Tao, F., Zhang, Z., Liu, J., Yokozawa, M., 2009. Modelling the impacts of weather and climate variability on crop productivity over a large area: a new super-ensemble-based probabilistic projection. Agric. For. Meteorol. 149 (8), 1266–1278. https://doi.org/10.1016/j.agrformet.2009.02.015.

Turco, M., Sanna, A., Herrera, S., Llasat, M.C., Gutiérrez, J.M., 2013. Large biases and inconsistent climate change signals in ENSEMBLES regional projections. Clim. Change 120 (4), 859–869. https://doi.org/10.1007/s10584-013-0844-y.

van Vuuren, D.P., Carter, T.R., 2014. Climate and socio-economic scenarios for climate change research and assessment: reconciling the new with the old. Clim. Change 122 (3), 415–429. https://doi.org/10.1007/s10584-013-0974-2.

Wang, J., Wang, E., Luo, Q., Kirby, M., 2009. Modelling the sensitivity of wheat growth and water balance to climate change in Southeast Australia. Clim. Change 96 (1–2), 79–96. https://doi.org/10.1007/s10584-009-9599-x.

Willmott, C.J., Ackleson, S.G., Davis, R.E., Feddema, J.J., Klink, K.M., Legates, D.R., Rowe, C.M., 1985. Statistics for the evaluation and comparison of models. J. Geophys. Res.: Oceans 90 (C5), 8995–9005. https://doi.org/10.1029/JC090iC05p08995.

Zhang, X.C., Liu, W.Z., Li, Z., Chen, J., 2011. Trend and uncertainty analysis of simulated climate change impacts with multiple GCMs and emission scenarios. Agric. For. Meteorol. 151 (10), 1297–1304. https://doi.org/10.1016/j.agrformet.2011.05.010.

Zhao, G., Bryan, B.A., Song, X., 2014. Sensitivity and uncertainty analysis of the APSIM-wheat model: Interactions between cultivar, environmental, and management parameters. Ecol. Model. 279, 1–11. https://doi.org/10.3390/agronomy10070981.